# Hidden Black Holes at High Redshift

J. Stuart B. Wyithe[1], Abraham Loeb[2]

[1] *School of Physics, University of Melbourne, Parkville, Victoria, Australia*
[2] *Astronomy Department, Harvard University, 60 Garden Street, Cambridge, MA 02138, USA*
*Email: swyithe@physics.unimelb.edu.au; aloeb@cfa.harvard.edu*

8 September 2011

**ABSTRACT**
Recent X-ray observations show evidence for substantial accretion onto central black holes in galaxies at $z > 6$, which is not reflected in optical output, suggesting that most black-hole mass at high redshift is accreted during an obscured phase and with high duty cycle. In this *Letter* we identify a physical mechanism that naturally leads to obscured growth in galaxies at $z > 6$. Specifically we find that the density at the centre of $z > 6$ reaches a level where the diffusion time of optical photons out to the Bondi accretion radius is expected to be longer than the gravitational free-fall time, so that they are trapped. We argue that the observed prevalance of obscured accretion indicates that black-holes are undergo an extended phase of very low efficiency accretion, providing a natural explaination the presence of super-massive black-holes at $z \sim 6 - 7$ less than a billion years after the Big Bang.

**Key words:** galaxies: evolution, formation, high-redshift — cosmology: theory

## 1 INTRODUCTION

Exceptionally bright quasars with redshifts up to $z \sim 7$ have recently been discovered (Mortlock et al. 2011). Quasars are thought to be powered by the accretion of gas onto super-massive black holes at the centres of galaxies. Their maximum (Eddington) luminosity depends on the mass of the black hole, and the brighter quasars are inferred to have black holes with masses of more than a few billion solar masses. Since their discovery (Fan et al 2002), the existence of such massive black holes at $z > 6$ has posed a challenge to models for their formation. This is because a $\sim 10^9 \mathrm{M}_\odot$ black-hole accreting with a radiative efficiency of 10% requires almost the full age of the Universe at $z \sim 6$ to grow from a stellar mass seed. Many authors have therefore discussed solutions to this apparent mystery by including a significant build-up of mass through mergers (reference from Haiman I think), or Super-Eddington Accretion (reference from Vollonteri & Rees I think).

Motivated by the recent discovery that most black-hole accretion at $z \gtrsim 6$ is optically obscured and in galaxies below halo masses of $\sim 10^{11} \mathrm{M}_\odot$, we identify an important physical mechanism that is expected to operate in the very dense centres of high redshift galaxies. Specifically, we find that at sufficiently high redshift the Bondi accretion rate exceeds the rate required to trap optical-UV radiation and advect it into the black-hole. We show that this required rate is several orders of magnitude larger than the Eddington accretion rate corresponding to an accretion efficiency of 10% which is typical for quasars. Since such an accretion

rate would drive a wind that would prevent the inflow from reaching a level where it would trap the radiation, we argue that the observation of obscured accretion implies that most super-massive black-hole mass is accreted at very low efficiency. This low efficiency allows the build-up of super-massive black-hole mass over a period that is several orders of magnitude shorter than the Hubble time.

We begin in § 2 with a description of our simple model, before presenting our results in §3 and discussion in § 4. In our numerical examples, we adopt the standard set of cosmological parameters Komatsu et al. (2011), with values of $\Omega_\mathrm{b} = 0.04$, $\Omega_\mathrm{m} = 0.24$ and $\Omega_\Lambda = 0.76$ for the matter, baryon, and dark energy fractional density respectively, $h = 0.73$, for the dimensionless Hubble constant, and $\sigma_8 = 0.82$.

## 2 MODEL

The basis of this *Letter* is a comparison between the Bondi accretion rate, and the accretion rate required to trap photons within the accretion flow. We discuss these in turn.

### 2.1 The Bondi accretion rate

We begin with the expression for the Bondi accretion rate onto a central black hole of mass $M_\mathrm{bh}$

$$\dot{M}_\mathrm{Bondi} = 4\pi \rho_0 r_\mathrm{b}^2 v_\mathrm{ff} = 4\pi n_0 \mu m_\mathrm{p} r_\mathrm{b}^2 \sqrt{\frac{GM_\mathrm{bh}}{r_\mathrm{b}}}, \qquad (1)$$

where $v_{ff}$ is the free-fall time at the Bondi radius

$$r_{\rm b} = \frac{GM_{\rm bh}}{c_{\rm s}^2}, \tag{2}$$

and $c_{\rm s}$ is the sound speed, which for an isothermal gas we assume corresponds to a temperature of $10^4$K. To evaluate $\dot{M}_{\rm Bondi}$ we need to specify the central number density of a self gravitating disk (Schaye 2004)

$$n_0 = \frac{GM_{\rm disk}^2}{12\pi c_{\rm s}^2 R_{\rm d}^4 \mu m_{\rm p}}. \tag{3}$$

Here $R_{\rm d}$ is the characteristic radius of an exponential disk of surface density profile

$$\Sigma = \Sigma_0 \exp(-r/R_d), \tag{4}$$

with $\Sigma_0 = M_{\rm disk}/2\pi R_d^2$, and the disk scale length is given by

$$R_d = \frac{\lambda}{\sqrt{2}} r_{\rm vir}, \tag{5}$$

where $\lambda = 0.05$ is the mean value for the dimensionless spin parameter of the halo. In equation (3) the disk mass $M_{\rm disk} = m_{\rm d}M$, $m_{\rm p}$ is the mass of hydrogen, and $\mu$ is the molecular weight. At the high redshifts of interest, most of the virialized galactic gas is expected to cool rapidly and assemble into the disk. We therefore assume $m_{\rm d} = 0.17$. The corresponding mass density is $\rho_0 = m_{\rm p}n_0$. The virial radius is given by the expression

$$r_{\rm vir} = 0.784 h^{-1} {\rm kpc} \left(\frac{M_{\rm halo}}{10^8 M_\odot h}\right)^{\frac{1}{3}} [\zeta(z)]^{\frac{-1}{3}} \left(\frac{(1+z)}{10}\right)^{-1},$$

where $\zeta(z)$ is close to unity and defined as $\zeta \equiv [(\Omega_m/\Omega_m^z)(\Delta_c/18\pi^2)]$, $\Omega_m^z \equiv [1 + (\Omega_\Lambda/\Omega_m)(1+z)^{-3}]^{-1}$, $\Delta_c = 18\pi^2 + 82d - 39d^2$, and $d = \Omega_m^z - 1$ (see equations 22–25 in Barkana & Loeb 2001 for more details). From equations (6) and (3) we see that the central density $n_0$, and hence the Bondi accretion rate $\dot{M}_{\rm Bondi}$ scales as $(1+z)^4$, and thus that accretion rates are expected to be much larger at high redshift.

Before proceeding, we note that our model places high redshift super-massive black-holes within the centre of a disk, whereas bulge-less disks at low redshift are not known to house black-holes. However, in the halos corresponding to high redshift drop-out galaxies at which we aim our model, the virial velocity and the sound speed (which sets the disk thickness) are similar in magnitude. Disks in these high redshift galaxies are therefore thick, with scale heights comparable to their radii.

Dormant SMBHs are ubiquitous in local galaxies (Magorrian et al. 1998). The masses of these SMBHs scale with physical properties of their hosts (e.g. Magorrian et al., 1998; Merritt & Ferrarese 2001; Tremaine et al. 2002). However at high redshift the relations observed in the local Universe may not be in place. We therefore do not impose a model for the relation between black-hole and halo mass in this paper, and instead explore a range of values. Indeed, our results indicate that feedback, which is thought to drive the black-hole – halo-mass relation relation, would not be effective at early times. The grey curves in Figure 1 show the Bondi accretion rate as a function of redshift for different values of halo and black-hole mass.

## 2.2 Photon trapping by the accretion flow

If the time for diffusion of photons out to a radius $r$ is longer than the free-fall time of the material from radius $r$, then photons become trapped in the accretion flow. In such cases, the black hole would be obscured in optical wavelengths. In this section we estimate the accretion rate required to achieve this photon trapping.

The free-fall time from radius $r$ is

$$t_{\rm ff} \sim \frac{r}{v_{\rm ff}}, \tag{6}$$

where $v_{\rm ff} \sim \sqrt{GM_{\rm bh}/r}$ within the Bondi radius. This should be compared with the diffusion time of

$$t_{\rm diff} \sim \tau \frac{r}{c}. \tag{7}$$

Here the optical depth is given by

$$\tau \sim \bar{\rho} \frac{F_{\rm sig} \sigma_{\rm T}}{m_{\rm p}} r, \tag{8}$$

where $\sigma_{\rm T}$ is the Thomson cross-section, $F_{\rm sig}$ is the ratio of the cross-section of the accreting gas to $\sigma_{\rm T}$, and $\bar{\rho}$ is the line-of-sight averaged density out to radius $r$. The density within the Bondi radius scales as $\rho(r) = \rho_0(r/r_{\rm b})^{-1.5}$. Assuming the cross-section to be dominated by dust, and a sublimation radius $r_{\rm sub}$ below which the cross-section per unit mass is two orders of magnitude lower, we find

$$\bar{\rho} = 2\rho_0 \frac{r_{\rm b}}{r - r_{\rm sub}} [(\frac{r_{\rm sub}}{r_{\rm b}})^{-0.5} - (\frac{r}{r_{\rm b}})^{-0.5}]$$
$$\qquad\qquad \text{if} \quad r < r_{\rm b}$$
$$\bar{\rho} = \frac{(r_{\rm b} - r_{\rm sub}) \left[2\rho_0 \frac{r_{\rm b}}{r_{\rm b} - r_{\rm sub}} [(\frac{r_{\rm sub}}{r_{\rm b}})^{-0.5} - 1]\right] + (r - r_{\rm b})\rho_0}{(r - r_{\rm sub})}$$
$$\qquad\qquad \text{if} \quad r > r_{\rm b}, \tag{9}$$

where we have taken $\rho = \rho_0$ at $r > r_{\rm b}$.

The condition $t_{\rm diff} > t_{\rm ff}$ at radius $r$ is satisfied for accretion rates

$$\dot{M}_{\rm lim} > \frac{\rho_0}{\bar{\rho}} \left(\frac{4\pi m_{\rm p}c}{F_{\rm sig}\sigma_{\rm T}}\right) r, \tag{10}$$

where we have used the relation $\dot{M}_{\rm lim} = 4\pi\rho r^2 v_{\rm ff}$. Since the Eddington accretion rate at an efficiency $\epsilon$ is $\dot{M}_{\rm Edd} = (4\pi GM_{\rm bh}m_{\rm p})/(c\sigma_{\rm T}\epsilon)$, we find

$$\dot{M}_{\rm lim} > \left(\frac{\epsilon}{F_{\rm sig}}\right) \left(\frac{r}{r_{\rm g}}\right) \left(\frac{\bar{\rho}}{\rho_0}\right)^{-1} \dot{M}_{\rm Edd}, \tag{11}$$

where $r_{\rm g} = GM_{\rm bh}/c^2$.

These limiting accretion rates are plotted in the left hand panels of Figure 1 (dark lines) for the case where the vertical structure of the disk is set by the sound speed of the gas. The *Upper* and *Lower* panels correspond to cases of halo masses of $M = 10^{10}{\rm M}_\odot$ and $M = 10^{11}{\rm M}_\odot$. The opacity of the gas could be larger than the Thomson opacity by as much as two or three orders of magnitude due to dust (Laor & Draine 1993). The broad emission lines of all quasars indicate super-solar metallicities, probably because star formation precedes the quasar activity. On the other hand, the diffusion time may be lessened if the gas is clumpy, corresponding to an effective opacity that is lowered. We show curves corresponding to cross-sections that are $F_{\rm sig} = 100$ times larger than the Thomson cross-section (additional cases are presented below).
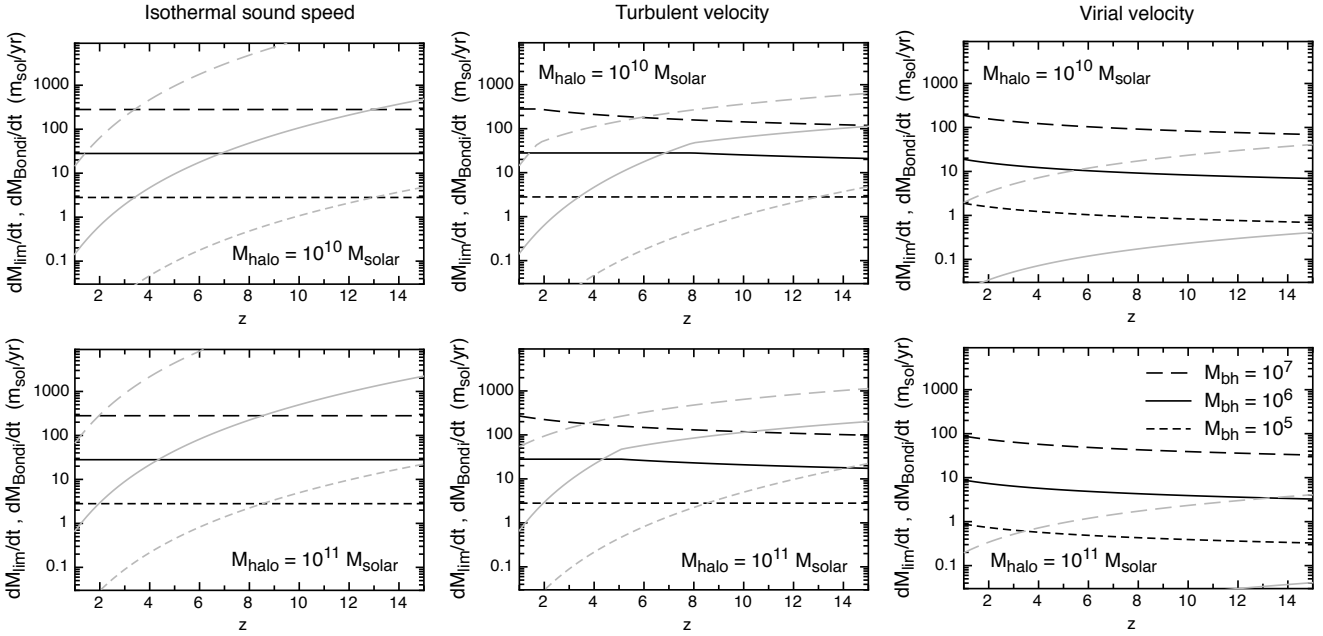
**Figure 1.** The grey curves show the accretion rate Bondi accretion rate as a function of redshift. The dark lines show the critical accretion rate for which the diffusion time out to the Bondi Radius to be longer than the gravitational free-fall time. In cases where the Bondi accretion rate is larger than the critical accretion rate, the photons are trapped and the quasar is obscured. Three cases are considered for the vertical structure of the disk, which is assumed to be set by the sound speed of the gas (*Left Panels:*), the turbulent velocity associated with a $Q = 1$ disk (*Central Panels:*), and the virial velocity (*Right Panels:*) respectively. In each case the *Upper* and *Lower* panels correspond to cases of halo masses of $M = 10^{10} M_\odot$ and $M = 10^{11} M_\odot$. Three curves in each case correspond to black-hole masses of $10^5 M_\odot$, $10^6 M_\odot$ and $10^7 M_\odot$. The cross-section was assumed to be $F_{sig} = 100$ times larger than the Thomson cross-section.

## 3  RESULTS

In cases where the Bondi accretion rate is larger than the critical accretion rate, the photons are trapped and the quasar is obscured. Thus the cross-over of the limiting and Bondi accretion rate curves in Figure 1 represents the redshift beyond which quasar activity would be obscured for the particular masses shown. Figure 1 shows that the more massive the black-hole, the lower the redshift above which it is obscured (at fixed halo mass and assuming constant values for $F_{sig}$ and $m_d$). This means that a small black-hole could begin obscured growth at high redshift, following which the obscuration continues as the black-hole grows towards low redshift. If the vertical disk structure is set by the sound speed, we find that a $10^6 M_\odot$ black hole in a $10^{10} M_\odot$ halo will be obscured at $z > 6$. This redshift is shown more clearly in Figure 2 which plots contours of the redshift at which the Bondi accretion rate becomes larger than the critical accretion rate as a function of halo and black-hole mass mass. This figure shows the mass combinations that give a cross over from non-obscured to obscured quasars. As already noted, at $z \sim 6 - 8$, this crossover should happen in galaxies with black-hole masses of $\sim 10^6 M_\odot$ in halos of $10^{10} M_\odot$.

### 3.1  Scaling relations

At a given redshift, the obscuration is more easily achieved for larger black-holes. This result follows from the scalings of free-fall and diffusion time (equations 6 and 7), which show $t_{ff} \propto r^{3/2}$ and $t_{diff} \propto r^2$, so that the ratio of diffusion time

to free-fall time is larger for more massive black holes which have a larger Bondi radius in galaxies of fixed mass.

The conditions for the halo mass, black hole mass, and redshift that conspire to provide accretion rates that trap the radiation can be obtained by combining equations (1) and (10), and evaluating at $r = r_b \gg r_{sub}$. We find

$$\frac{\dot{M}_{bondi}}{\dot{M}_{lim}} \sim 0.5 \left( \frac{M_{bh}}{10^6 M_\odot} \right) \left( \frac{M_{halo}}{10^{10} M_\odot} \right)^{2/3} \left( \frac{1+z}{7} \right)^4 \left( \frac{F_{sig}}{10} \right)$$
$$\left( \frac{m_d}{0.17} \right)^2 \left( \frac{F_{sub}}{10^4} \right)^{-1/2} \left( \frac{c_s}{10\,km/s} \right)^{-4} \left( \frac{\lambda}{0.05} \right)^{-4}, (12)$$

where we have related the sublimation radius to the gravitational radius through $r_{sub} = F_{sub} r_g$. This expression makes explicit the dependencies that lead to photons being more easily trapped (i.e. $\dot{M}_{bondi}/\dot{M}_{lim} > 1$) around larger black-holes in larger halos, and at higher redshift. Black-holes in excess of $10^6 M_\odot$ within halos of mass $10^{10} M_\odot$ or larger are obscured at $z \gtrsim 6$.

Similarly, the relation between the limiting rate for photon trapping and the Eddington rate can be illustrated via the condition

$$\frac{\dot{M}_{lim}}{\dot{M}_{Edd}} \sim 1.5 \times 10^3 \left( \frac{\epsilon}{0.1} \right) \left( \frac{F_{sig}}{10^2} \right)^{-1} \left( \frac{F_{sub}}{10^4} \right)^{0.5} \left( \frac{c_s}{10\,km/s} \right)^{-1}.$$
$$(13)$$

Thus an accretion rate that leads to photon trapping must be associated with accretion onto the black hole that is far in excess of the Eddington rate for a thin accretion disk ($\epsilon \sim 10\%$), and hence with a very rapid build-up of black-hole mass. Equation (13) therefore suggests that the obscured accretion observed in high redshift galaxies by Treister et
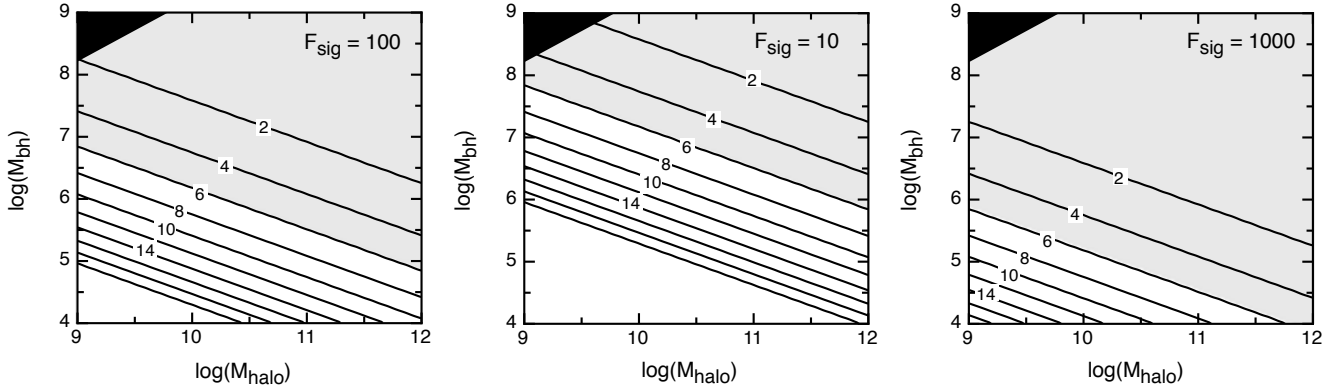
**Figure 2.** Contours of the redshift at which the Bondi accretion rate becomes larger than the critical accretion rate as a function of halo and black-hole mass. This shows the parameter combinations that give a cross over from non-obscured to obscured quasars (or from low to high duty-cycle). We show contours for cases where the vertical structure of the disk is assumed to be set by the sound speed of the gas. In the *Left*, *Central* and *Right* panels we show contours for opacities which are $F_{sig} = 100$ $F_{sig} = 10$ and $F_{sig} = 1000$ times larger than the Thomson cross-section. The grey regions show the obscured portion of parameter space at $z \sim 6$. The black areas show unphysical regions with $M_{bh} > m_d M$.

al. (2011) provides evidence for low high accretion rates at low efficiency ($\epsilon \ll 10\%$).

### 3.2  Disk structure

In the previous section we have assumed that the thickness of the disk in its centre is set by the sound speed of gas at $10^4$K. However in turbulent disks, the turbulent velocity replaces the role of the sound speed. Recently, Genzel et al. (200?) inferred a Toomre's Q value of $Q = 1$ in ULIRGS, implying a value for the turbulent velocity of $c_T \sim G\Sigma/\Omega = \sqrt{G\Sigma_0 r/\pi}$, where $v^2 = G\Sigma_0\pi r^2/r$ yielding $\Omega = v/r = \sqrt{G\Sigma_0\pi/r}$. Evaluating at the Bondi radius, we get

$$c_T = \left( \frac{G^2\Sigma_0 M_{bh}}{\pi} \right)^{0.25} \tag{14}$$

This value of $c_T$ is the maximum value possible for a disk at large radius (as a higher $c_T$ would imply an unphysical disk with $h > r$). Therefore, for $Q = 1$ disk the turbulent velocity should decrease towards small $r$. At sufficiently small radii, $c_T < c_s$, implying that the minimum thickness of the disk at its centre is set by the sound speed in the gas. We find that when evaluated at the Bondi radius, the turbulent velocity is smaller than the sound at high redshift unless the halo is very massive ($\gtrsim 10^{11}$ at $z > 4$).

There may also be sources of energy injection that heat the gas to temperatures that correspond to velocities much larger than $c_T$ (or $c_s$), although in order to remain bound the velocity of the gas must be smaller than the virial velocity of the halo. We therefore show two cases in addition to $c_s \sim$ 10km/s, namely $c_T$ and $c_v \sim f v_{vir}$ where $f \sim 0.5$ in order to bracket the range of interest, with corresponding limiting accretion rates plotted in the central and right hand panels of Figure 1 (dark lines). The results are almost unchanged where $c_T$ is used to set the disk height, since it is generally smaller than $c_s$ at the bondi-radius. However if the disk height is set by the maximum velocity $v_c$, then larger black-holes are needed in order for the Bondi accretion rate

to exceed the limiting rate, and at $z \sim 6$ black-hole accretion would not be obscured in this case.

### 3.3  Dependence on Opacity

In the *Central* and *Right* panels of Figure 2 we show contours for cases where the effective opacity of the gas is assumed to be $F_{sig} = 10$ and $F_{sig} = 1000$ times larger than the Thomson cross-section respectively. Smaller (larger) values of $F_{sig}$ lead to larger (smaller) inflow rates being needed to trap the radiation, and so larger (smaller) black-holes are needed before accretion becomes obscured at fixed halo mass and redshift (see equation 13). However even with $F_{sig} = 10$, a $10^6 M_\odot$ black hole in a $10^{10} M_\odot$ halo would be obscured at $z \gtrsim 7$.

### 4  DISCUSSION

Our results may be used to explain the observation in Treister et al. (2011) that Ly-break galaxies at $z \sim 6$ exhibit obscured accretion with a high duty cycle, as evidenced by X-rays, but with no corresponding rest-frame UV flux. In particular we find that at $z > 6$, galaxies with masses corresponding to those of the observed Ly-break population exhibit a Bondi-accretion rate that is sufficiently high to trap the optical radiation. This behaviour also fits with observations up to redshift 3 that optically obscured quasars are more common at higher redshift. On the other hand our model does not explain why optically obscured quasars are more common in lower mass systems, although we have not included halo mass-dependent gas mass-fractions or $F_{sig}$. For example, equation (13) describes a steep dependence of the obscuration on $m_d$ which might be expected to decrease in larger systems.

Our results point to some important implications for the growth of high redshift black-holes. A plausible scenario which is consistent with observations includes two episodes of black-hole growth. Initially the accretion may be at low

efficiency ($\lesssim 10^{-3}$), so that the Eddington rate is not exceeded by the inflow. In this case radiation can be trapped by the very large Bondi accretion rates that are possible at high redshift, and advected into the central black-hole. This phase of growth would be obscured at optical wavelengths. However if the gas settles into an accretion disk within the sublimation radius, then the accretion efficiency would be large ($\sim 10\%$), and a wind would be launched which would halt the large accretion rate at the Bondi radius (since the inflow and out-flow rates would be comparable, but the out-flow velocity would be much larger than the free-fall velocity).

During the obscured phase, the Bondi accretion rates in these high redshift galaxies would be several orders of magnitude larger than the Eddington rate corresponding to an efficiency of $\eta = 0.1$. This helps alleviate the difficulty of growing super-massive black-holes of more than a billion solar masses (corresponding to the most distant known quasars, Mortlock et al. 2011) within the first billion years of the Universe's age. To illustrate we note that accretion at the Eddington rate (with $\eta = 0.1$) leads to an e-folding time of $t = 4 \times 10^7$ years. Assuming that a black-hole accretes with a duty cycle of unity, the number of e-folding times available by $z \sim 7$ is therefore $\sim 20$. This should be compared with the 20 e-folds needed to grow a 1 solar mass black-hole seed up to a mass of $10^9$ solar masses. Thus there is only just enough time in the age of the Universe for a stellar black-hole seed to grow to a super-massive black-hole. Based on the calculations of this paper, we argue that the period of obscured growth (as indicated by X-ray observations of distant galaxies, Treister et al. 2011) would provide most of the mass of these super-massive black-holes. From Equation (13) we find that the number of e-folds available during the obscured phase would be several orders of magnitude larger, indicating that super-massive black-holes at $z \sim 6$ could complete their growth within 1% of the age of the Universe.

**REFERENCES**

Bouwens, R. J., et al. 2010, arXiv:1006.4360
Bouwens, R. J., Illingworth, G. D., Blakeslee, J. P., Broadhurst, T. J., & Franx, M. 2004, ApJL, 611, L1
Dekel, A., & Woo, J. 2003, MNRAS, 344, 1131
Ferguson, H. C., et al. 2004, ApJL, 600, L107
Hansen, Carl J.; Kawaler, Steven D. (1994). Stellar Interiors: Physical Principles, Structure, and Evolution. Birkhuser. p. 28. ISBN 038794138X.
Hathi, N. P., Jansen, R. A., Windhorst, R. A., Cohen, S. H., Keel, W. C., Corbin, M. R., & Ryan, R. E., Jr. 2008, AJ, 135, 156
Kennicutt, R. C., Jr. 1998, ApJ, 498, 541
Komatsu, E., et al. 2009, ApJS, 180, 330
McLure, R. J., Cirasuolo, M., Dunlop, J. S., Foucaud, S., & Almaini, O. 2009, MNRAS, 395, 2196
Mo, H. J., Mao, S.,& White, S. D. M. 1998, MNRAS, 295, 319

Muñoz, J. A., & Loeb, A. 2010, arXiv:1010.2260
Oesch, P. A., et al. 2010, ApJL, 709, L21
Raičević, M., Theuns, T., & Lacey, C. 2010, arXiv:1008.1785
Salvaterra, R., Ferrara, A., & Dayal, P. 2010, arXiv:1003.3873
Scalo, J. M. 1986, Fund. Cosmic Phys., 11, 1
Trenti, M., Stiavelli, M., Bouwens, R. J., Oesch, P., Shull, J. M., Illingworth, G. D., Bradley, L. D., & Carollo, C. M. 2010, ApJL, 714, L202
Windhorst, R. A., Hathi, N. P., Cohen, S. H., Jansen, R. A., Kawata, D., Driver, S. P., & Gibson, B. 2008, Advances in Space Research, 41, 1965
Windhorst, R. A., et al. 2010, arXiv:1005.2776
Wyithe, J. S. B., & Loeb, A. 2003, ApJ, 595, 614
Yan, H.-J., Windhorst, R. A., Hathi, N. P., Cohen, S. H., Ryan, R. E., O'Connell, R. W., & McCarthy, P. J. 2010, Research in Astronomy and Astrophysics, 10, 867